Supplemental Information

Characterization of Mg-based Bimetal Treatment of Insensitive Munition 2,4-dinitroanisole

Emese Hadnagy[1,*], Andrew Mai[2], Benjamin Smolinski[3], Washington Braida[2], Agamemnon Koutsospyros[1]

Submitted to:

Environmental Science and Pollution Research

[*]Corresponding Author. *Email address:* EHadnagy@newhaven.edu
[1]Department of Civil and Environmental Engineering, University of New Haven
[2]Department of Civil, Environmental, and Ocean Engineering, Stevens Institute of Technology
[3]RDECOM-ARDEC

Table S.1 Elemental Compositions (% Mass) of Bimetal Surfaces

Bimetal		O	Mg	Cu, Ni or Zn
Mg/Cu	Unused	53.1	34.7	12.2
	Used	65.6	34.4	0.6
Mg/Ni	Unused	44.7	14.7	40.6
	Used	54.4	18.8	26.8
Mg/Zn	Unused	41.9	23.4	34.7
	Used	53.8	31.5	14.7

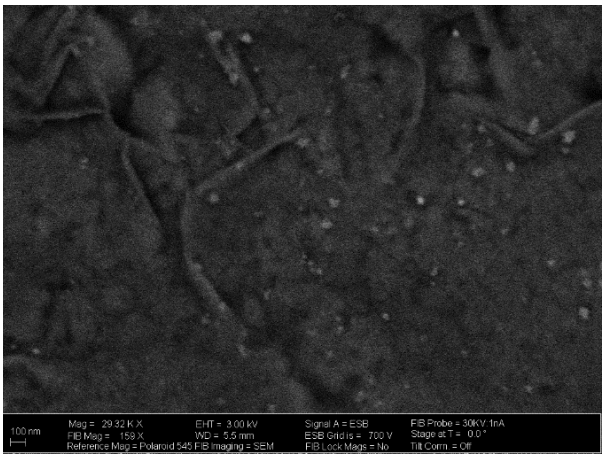

Fig. S.1 Contrasted SEM image of sample surface of unused Mg/Cu to more easily observe Cu nanoparticles

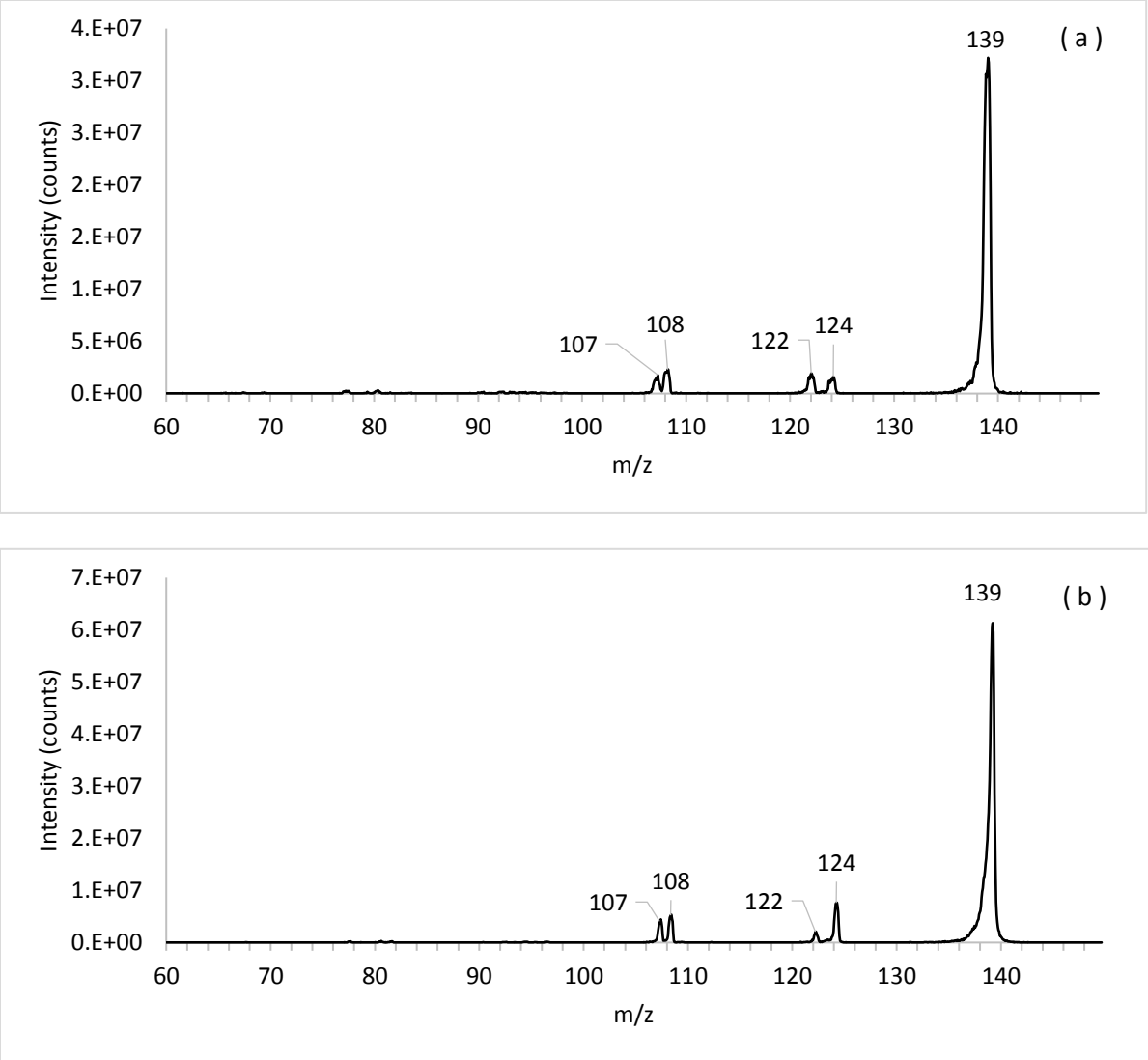

Fig. S.2 Daughter spectrum of m/z 139 from ESI-MS/MS in positive mode from (a) after DNAN treatment (solvent matrix, 0.5% S/L, 10:1 Mg to Cu ratio and 2.5 hr treatment) and (b) pure DAAN solution reference

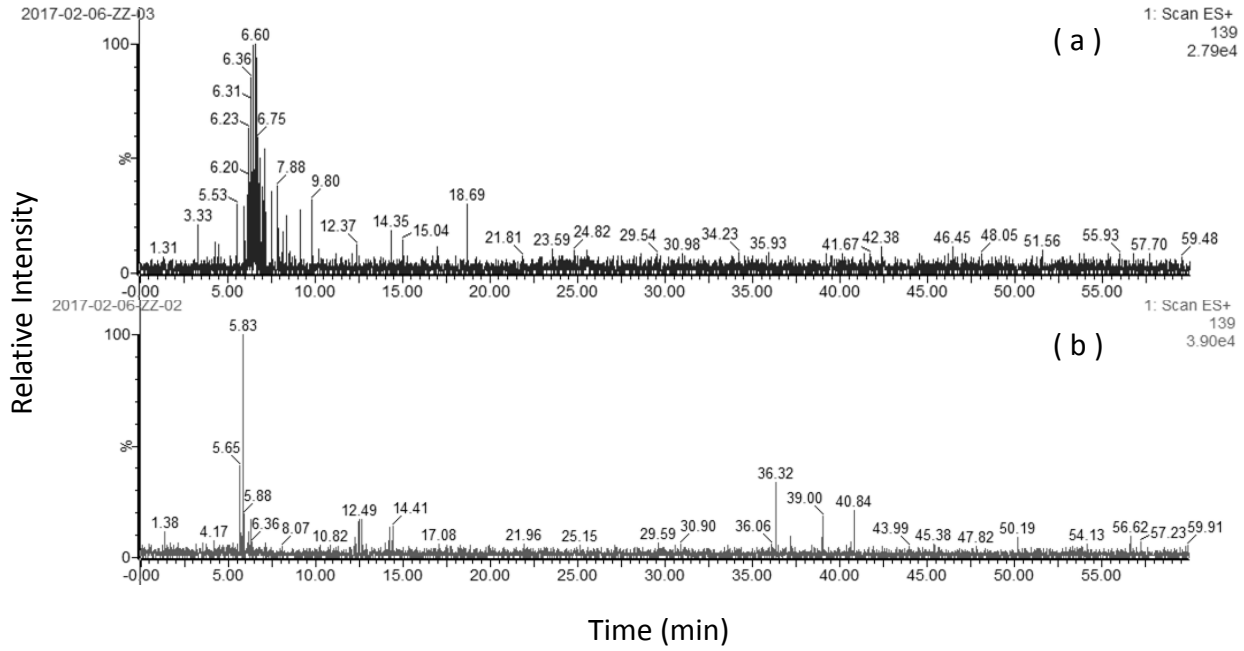

Fig. S. 3 Mass chromatograms of selected ion m/z 139 obtained from HPLC-ESI-MS of (a) pure DAAN, and (b) treated 4-ANAN sample (aqueous solution, 0.5% S/L, 10:1 Mg to Cu ratio and 1 hr treatment) where the elution of m/z 139 was identical. The slight difference in elution times (<1min) was due to peak shifts on HPLC

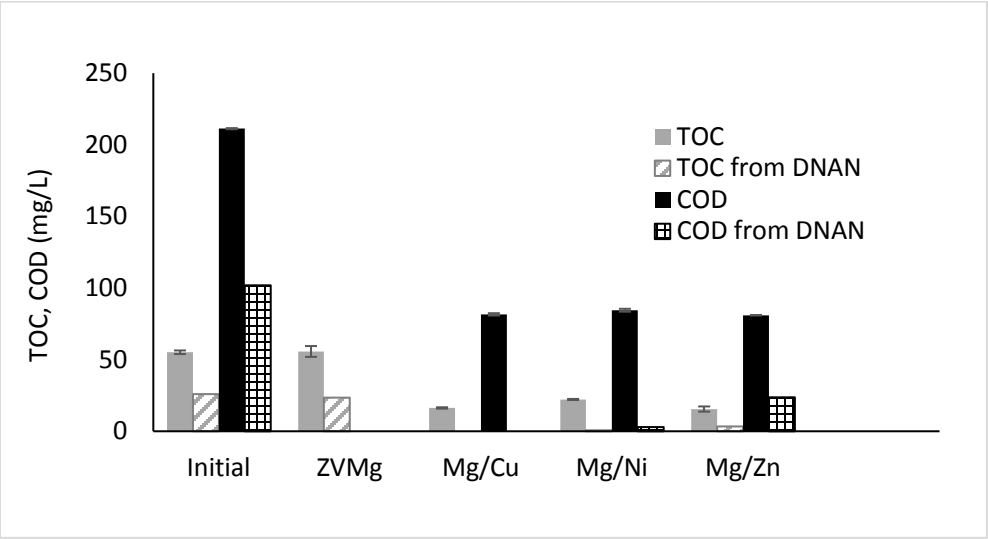

Fig. S.4 TOC, COD (mg L^{-1}) and DNAN contribution to TOC and COD in treated wastewater (0.5% S/L, 10:1 Mg to catalytic metal ratio, and 2.5 h treatment time, COD not measured for ZVMg)

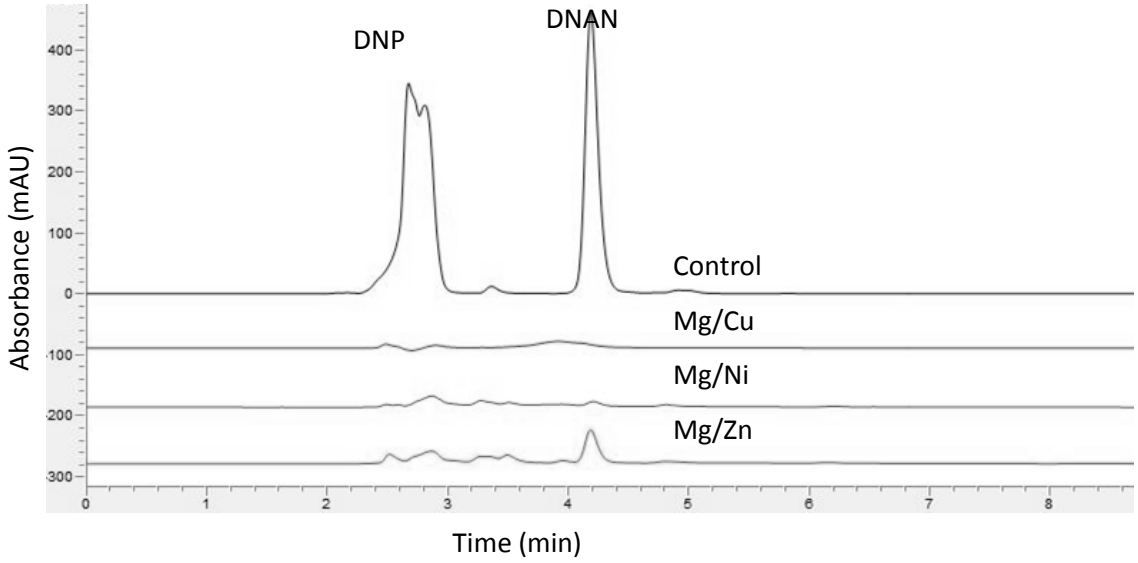

Fig. S.5 Visualization of degradation of DNP (2.1 min) and DNAN (4.2 min) in the wastewater control (top chromatogram) versus wastewater treated with Mg/Cu, Mg/Ni and Mg/Zn using overlaid chromatograms after 150 minutes of treatment (wastewater matrix, 0.5% S/L, 10:1 Mg to secondary metal ratio)

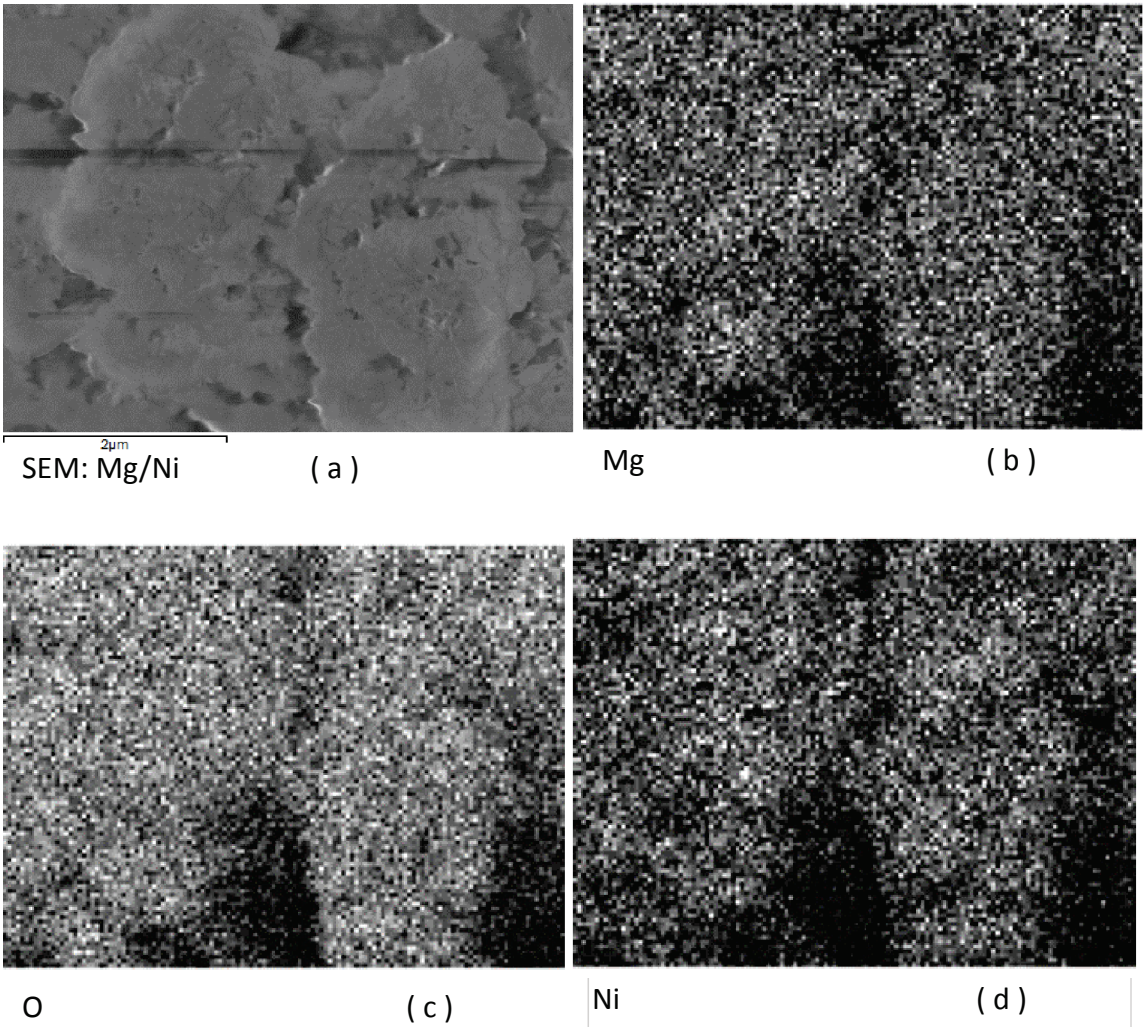

Fig. S.6 EDS mapping of (a) sample region of an unused particle of Mg/Ni pictured by SEM elucidating distribution of (b) primary metal Mg to (c) oxygen, and (d) catalytic metal Ni

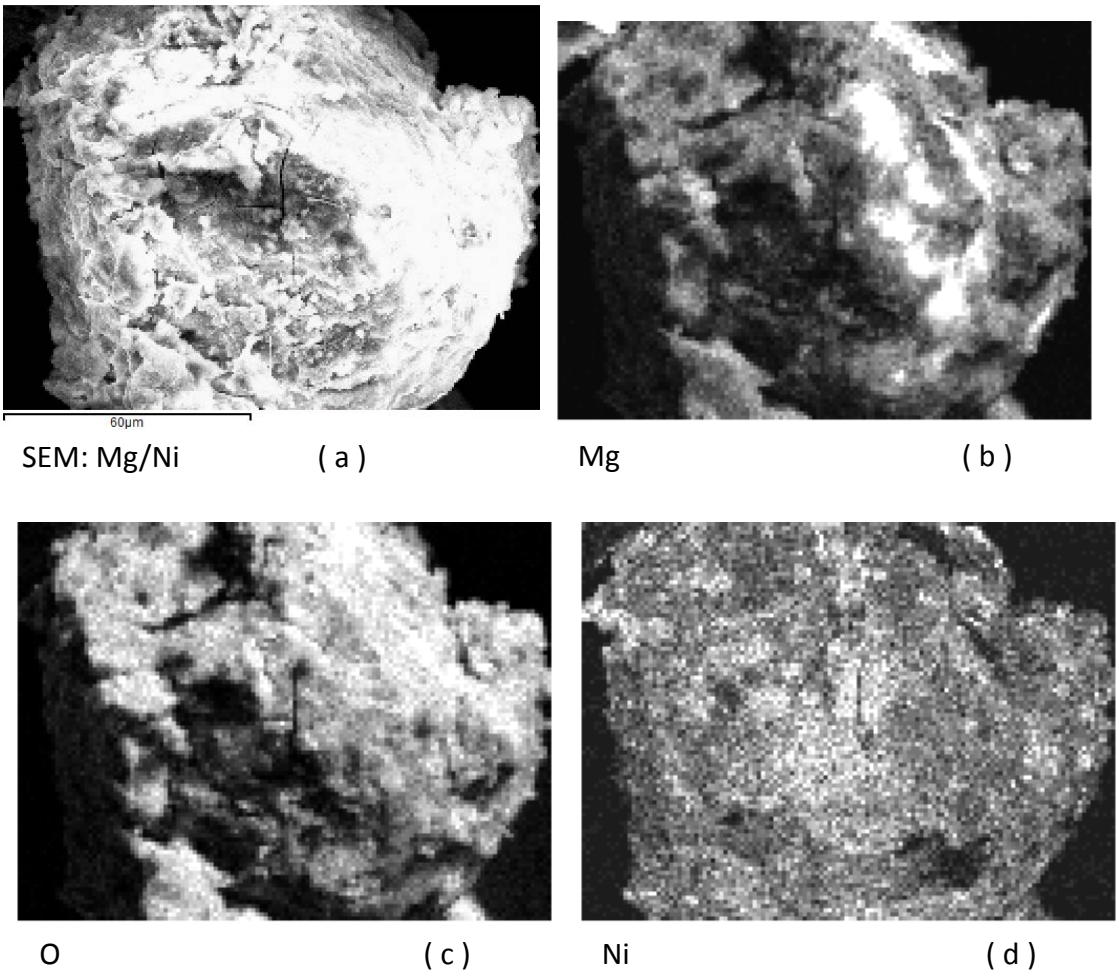

Fig. S.7 EDS mapping of (a) sample region of a used particle of Mg/Ni pictured by SEM elucidating distribution of (b) primary metal Mg to (c) oxygen, and (d) catalytic metal Ni

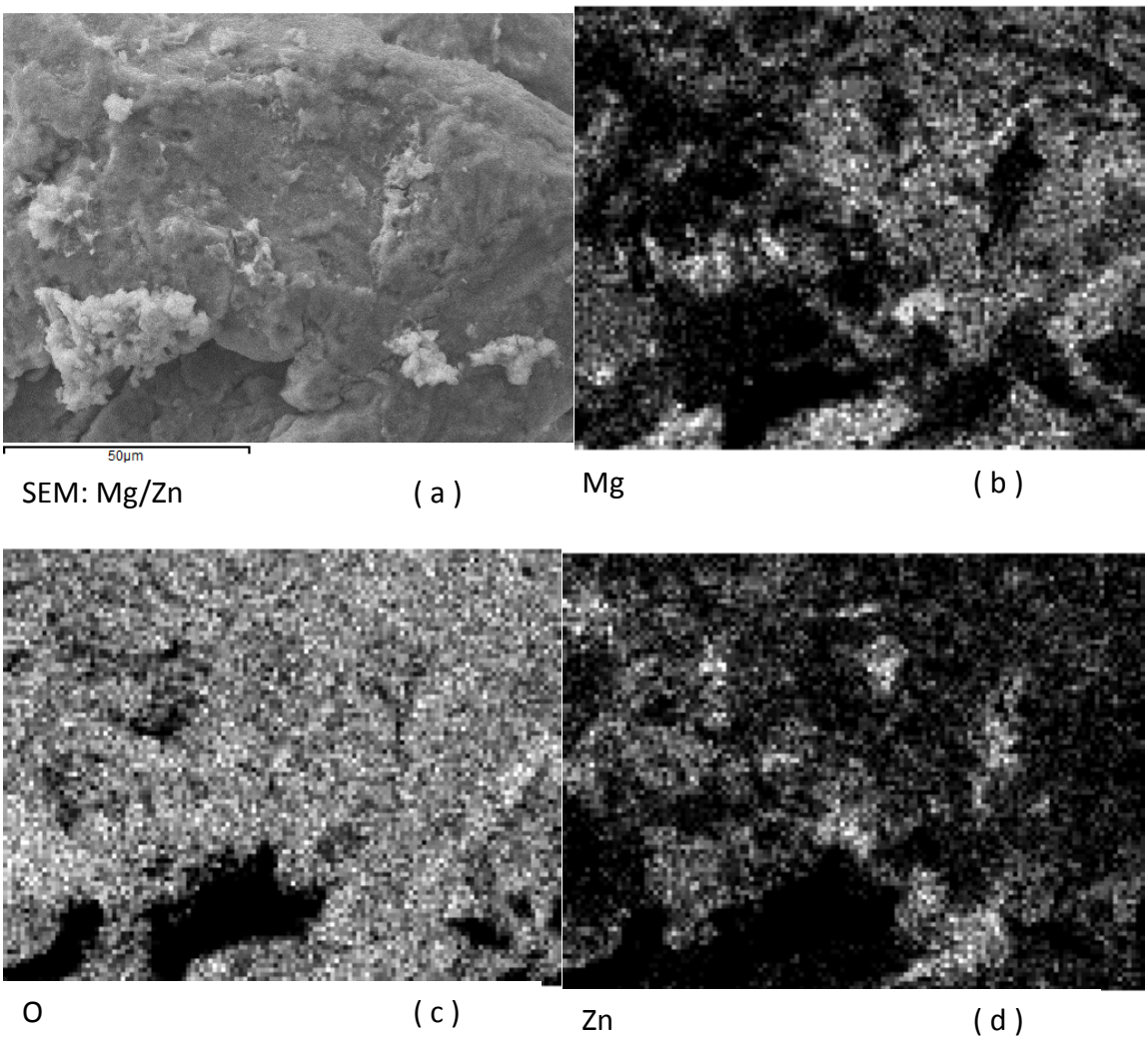

Fig. S.8 EDS mapping of (a) sample region of an unused particle of Mg/Zn pictured by SEM elucidating distribution of (b) primary metal Mg to (c) oxygen, and (d) catalytic metal Zn

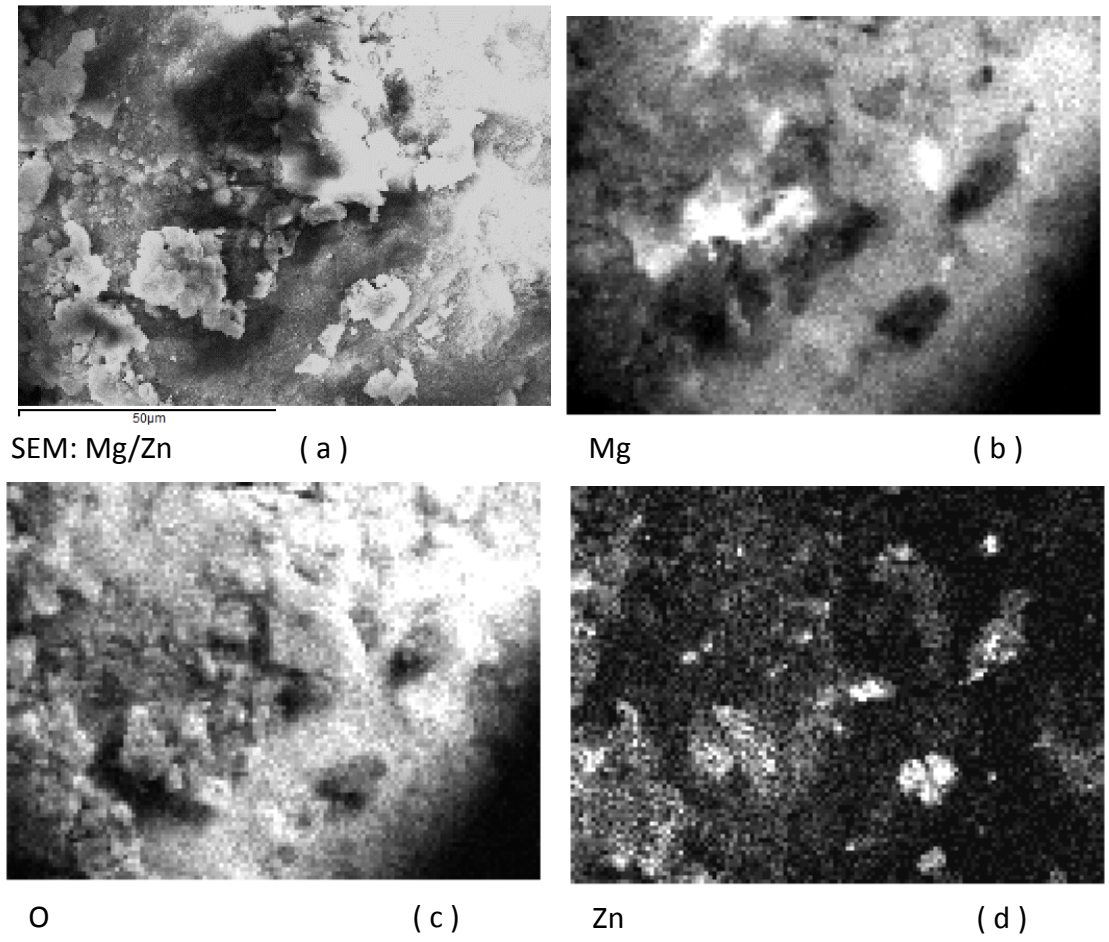

Fig. S.9 EDS mapping of (a) sample region of a used particle of Mg/Zn pictured by SEM elucidating distribution of (b) primary metal Mg to (c) oxygen, and (d) catalytic metal Zn

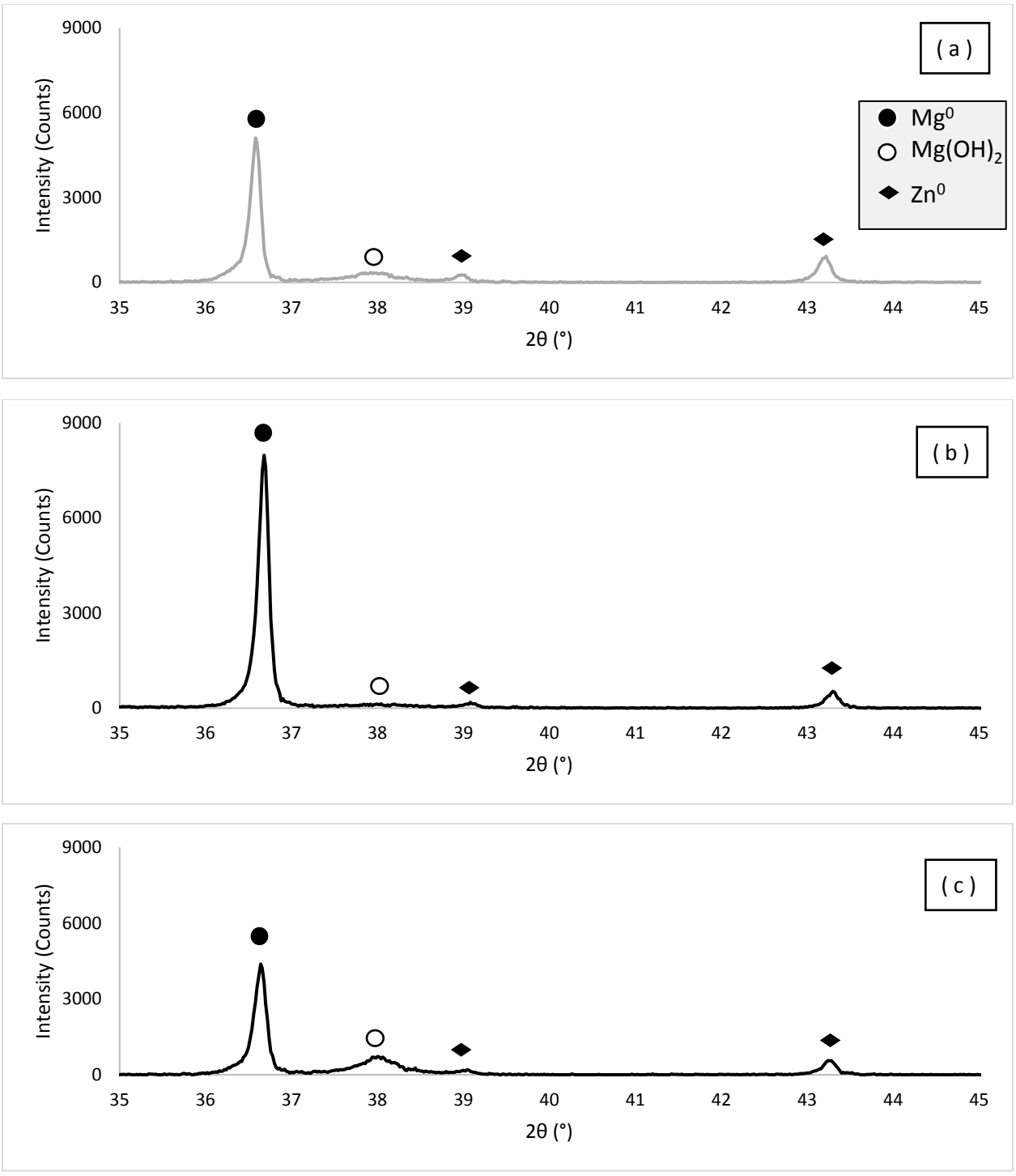

Fig. S.10 XRD patterns of Mg/Zn (a) before treatment, (b) after treatment in wastewater, (c) and after treatment in the pure aqueous phase

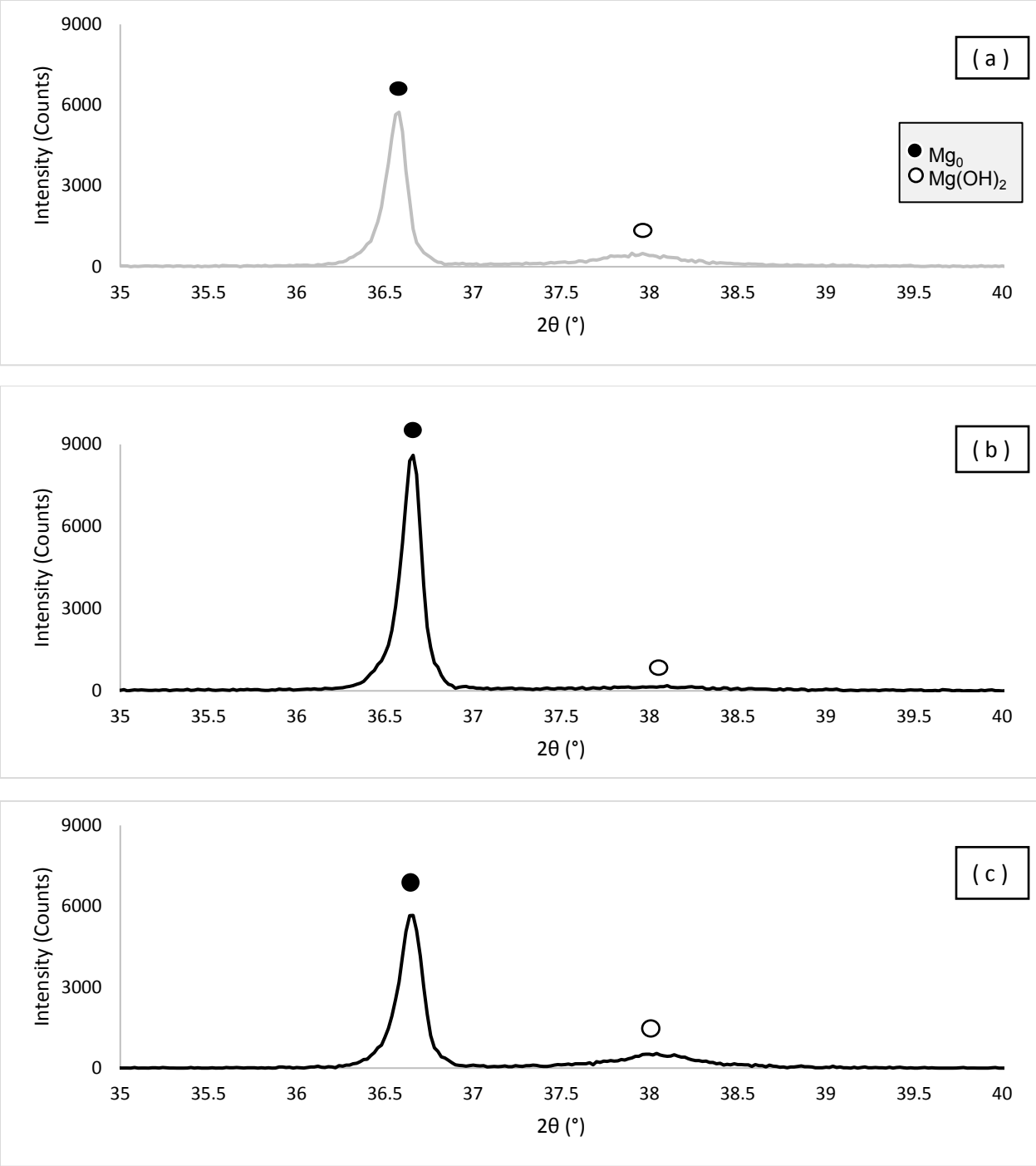

Fig. S.11 XRD patterns of Mg/Ni (a) before treatment, (b) after treatment in wastewater, and (c) after treatment in the pure aqueous phase